A zebrafish retinal graded photochemical stress model

Article *in* Journal of Pharmacological and Toxicological Methods · April 2009

DOI: 10.1016/j.vascn.2009.02.006 · Source: PubMed

4 authors, including:

Joseph Eichenbaum
Icahn School of Medicine at Mount Sinai
31 PUBLICATIONS **357** CITATIONS

SEE PROFILE

Published in final edited form as:
J Pharmacol Toxicol Methods. 2009 ; 59(3): . doi:10.1016/j.vascn.2009.02.006.

A zebrafish retinal graded photochemical stress model

Joseph W. Eichenbaum[a,b,*], **Ayca Cinaroglu**[c], **Kenneth D. Eichenbaum**[d], and **Kirsten C. Sadler**[c]

[a]Department of Ophthalmology, Mount Sinai School of Medicine, United States

[b]Department of Pharmacology, New York University School of Medicine, United States

[c]Department of Medicine, Division of Liver Disease and Department of Developmental and Regenerative Biology, Mount Sinai School of Medicine, United States

[d]Department of Structural and Chemical Biology, Mount Sinai School of Medicine, United States

Abstract

Introduction—In order to develop a model for investigating the genes that contribute to retinal degeneration, we examined the early graded photochemical stress response in the adult zebrafish (*Danio rerio*) retina and investigated the role of an NMDA inhibitor, thiokynurenate.

Methods—Following intravitreal injection of rose bengal (6 or 12 mg/mL), light (37×10^3 or 83×10^3 lx) was directed onto the central retina with and without 400 nM thiokynurenate. Histologic and electron microscopic analysis was performed at 2 and 4 h and gene expression analysis was carried out at 2, 4 and 6 h.

Results—Light and electron microscopy demonstrated a graded photochemical response in photoreceptor, nuclear, and ganglion cell layer thickness. Increased vacuolation of the inner plexiform layer was also observed. The inhibitor produced a distinct lesion pattern. Cellular stress genes were elevated in low and high lesions, while some homeobox gene expression was reduced with thiokynurenate.

Discussion—The phenotypic and genetic changes observed from this model can serve as a basis for understanding the pathology of retinal oxidative and cellular stress. These changes may aid our understanding of aging and macular degeneration.

Keywords

Photochemical cellular stress; NMDA inhibitor; Genes in retinal degeneration; Zebrafish

1. Introduction

Oxidative stress, often related to photochemical damage, is one of the leading causes of macular degeneration. The abundance of rods and four different types of cones in the zebrafish retina provide a fertile platform for examining oxidative stress. By creating photochemical oxidative stress utilizing rose bengal and light, we examined structural, ultra-structural, and gene expression changes in the retina of adult zebrafish.

Rose bengal deposited within the extracellular space and exposure to white light produces degenerative features in irradiated retinal neurons and its axons (Picaud, Peichl, &

*Corresponding author.1050 Park Avenue, New York, NY 10028, United States. Tel.: +1 212 289 7200; fax: +1 212 289 7474. Joseph.Eichenbaum@mssm.edu (J.W. Eichenbaum).

Franceschini, 1993). Studies involving the combination of rose bengal and light exposure have also demonstrated the capability to produce small cortical strokes in mice and rats (Eichenbaum et al., 2002; Pevsner et al., 2001). Rose bengal dye kinetics, measured by fluorescent microscopy, detected fluorescence in the retinal pigment epithelium of the rabbit at 5 min, mildly increased over the next 15 min and began acting in the inner retina at 60 min (Haimovici et al., 2002). Retinal photodegeneration lesions induced by rose bengal in the rat retina showed macrophages invaded the damaged retinae within a day (Picaud et al., 1993). Rose bengal intravitreous injection combined with light has been successfully used in dogs to generate free radical injury, a spectrum of Retinopathy of Prematurity, fibrovascular proliferation with retinal traction, retinal vascular peripheral vascularization and dilation, shunt vessels, retinal detachment, and vitreous hemorrhage and retinal dysplasia (Sadda et al., 1994). Therefore, light activated rose bengal serves as a useful method to induce lesions in the retina that may serve as a model for studying the pathophysiology of macular degeneration.

The exact mechanism by which rose bengal induces retinal damage is not clear. Photochemical lesions of the rat retina, very similar to high glutamate or aspartate exposure, (Mosinger & Olney, 1989; Olney, 1969) produced significant choline acetyltransferase and glutamic acid decarboxylase activity reductions, suggesting neurotoxicity of cholinergic and GABAergic retinal neurons (Moroni, Lombardi, Pellegrini-Faussone, & Moroni, 1993). Thiokynurenate is an antagonist of the glycine site of the N-methyl-D-aspartate (NMDA) receptor and has also been shown to block lipid peroxidation (Moroni et al., 1991, 1992). Interestingly, a single 400 nmol intravitreal injection of thiokynurenate immediately after a photochemical lesion was induced in rat retinas protected the outer and inner retina from ischemic retinal cell damage as assessed by ultrastructural studies (Matini, Moroni, Lombardi, Faussone-Pellegrini, & Moroni, 1997). This suggests that either signaling through the NMDA receptor or oxidative stress induced by lipid peroxidation may serve as the mechanistic basis for retinal damage caused by rose bengal and light.

A major drawback to using mammalian models to study retinal degeneration is the financial and time investment required to investigate the genes that are responsible for predisposition to this disease. Zebrafish provide a useful model to carry out forward genetic screens to identify genes required for retinal development (Gross et al., 2005; Malicki et al., 1996; Wehman, Staub, Meyers, Raymond, & Baier, 2005). Additionally, adult zebrafish have recently been reported as a useful system to study retinal degeneration (Cao, Jensen, Soll, Hauptmann, & Cao, 2008; Kassen et al., 2007; Liu & Londraville, 2003; Vihtelic & Hyde, 2000).

We therefore took advantage of this genetically tractable vertebrate to develop a model of retinal degeneration induced by oxidative stress.

If photochemically induced damage causes oxidative stress, then a select group of genes, including *sod*, *bip* (Gulow, Bienert, & Haas, 2002), *chop* (Horibe & Hoogenraad, 2007) and homeobox genes, may serve as early markers of the cellular stress in the retina. In this study, after a brief photochemical exposure, a significant phenotypic and gene expression changes were demonstrated in zebrafish. Such change can serve as a framework for understanding retinal degenerative disease.

2. Materials and methods

2.1. Animal care committee, fish care and maintenance

Wild-type adult 1–3 years old zebrafish were maintained in either the NYU Skirball Institute for Molecular Biology or Mount Sinai School of Medicine zebrafish facility on a 11/13 or

10/14 light dark cycle and reared at 28 C according to standard procedures. All procedures were approved by the Mount Sinai Institutional Animal Care and Use Committee.

2.2. Anesthesia technique

Tricaine (ethyl 3-aminobenzoate methane sulfonate salt), Sigma A5040S6 was dissolved at 266 mg/L of fish water pH 7.1–7.2. Anesthetic technique was followed according to a standardized protocol (Westerfield, 1995). Sponge/salt water bath operative platform were used.

2.3. Rose bengal treatment

For all experiments the right eye of each zebrafish was experimental and the left eye served as the control. In total, 126 fish (half males, half females) were used: 66 experimental, 60 controls with 6 fish per group.

2.3.1. Rose bengal preparation and intravitreal injection—Rose Glo™, rose bengal sterile ophthalmic strips, 1.5 mg/strip, (Rose Stone Enterprises, Alta Loma CA), were used to prepare either 6.0 mg/mL or 12 mg/mL rose bengal in distilled water for intravitreal injection. Microliter® #62 gauge (Hamilton Co., Reno NV), syringe and needle, 33GARN-37 30DEG, were used to inject 1 μL of rose bengal intravitreally under microscopic control (Mentor microscope, CMIII, Randolph Mass.). The injection was on the caudal side of the globe just behind the ciliary body near the 9 o'clock limbus.

2.4. Fiberoptic source, light meter

Gossen Mavolux 5032C light meter, (Germany), was used to measure the luminance in lux of the Volpi Intralux 5000 cold white coherent fiberoptic light, (120 V, 185 W, 50/60 Hz, Switzerland), which was previously calibrated to achieve either low 37×10^3 lx or high 83×10^3 lx exposure. After confirming the light energy level with the light meter, the fiberoptic cable was placed into the water bath over the cornea.

The time of the lesion induction from removal of the fish from the anesthetic tank to completion of the luminance was under 5 min. Fish breathing and heartbeat were easily monitored through the microscope.

2.5. Exposures

Experiments were performed as described in Table 1: Experimental design. Following treatment, all fish were transferred to a post-operative tank where they swam for 2, 4, or 6 hours under usual light adaptation conditions and were then euthanized with standard tricaine protocol.

2.6. Enucleation, histopathologic, and EM preparation

At the conclusion of either rose bengal and light exposure, rose bengal alone, light alone, or no treatment, the fish eyes were enucleated with jeweler's forceps and iris scissors. The globes were fixed in 4% paraformaldehyde (Sigma), for 40 min and then stored in Phosphate Buffered Saline at 4 °C until processing for paraffin embedding and staining with hematoxylin and eosin according to protocol (Dezna, Sheehan, & H.B., 1980).

At 2, 4 and 6 h after experimental exposures, fish were anesthetized and the front third of the globes were excised with iris scissors and jeweler's forceps leaving just the retina, choroid, and sclera, having removed cornea, iris, lens, and vitreous. The retina was then separated together with the pigment epithelium away from the choroid and fixed in 3% glutaraldehyde and processed for transmission electron microscope (EM).

2.7. Thiokynurenate intravitreal injection

7-chlorothiokynurenic acid, molecular weight 276.13 was kindly provided by Dr. Pelliciari, Department of Chemistry, Technology, and Pharmacology, Perugia, Italy. One microliter of 400 nmol was injected intravitreally, immediately after the Rose Bengal light lesion through the same injection site as the rose bengal. The fish were allowed to recover for 2–4 h and then the fish were re-anesthetized and underwent either enucleation for light microscopy or retinal dissection for electron microscopy and RNA extraction.

2.8. Measurements of retinal layers and gene expression

Measurements of the retinal layers in each of the experimental groups were made using the Olympus DP70 camera software. Six measurements were made for each retinal layer, averaged and standard deviation was obtained. The Student's *T*-test, which requires uniform variances, could not be applied because the variances vary from distribution to distribution. Therefore, we elected to calculate standard deviation as a statistical method. We calculated *p*-values, which were derived from the standard deviation between the two measurements as calculated by the equation: $\sqrt{\left(\sigma_A^2+\sigma_B^2\right)}$ where *A* and *B* were each retinal layer length measurement respectively. *p*-value measurements were calculated using standard 95% confidence intervals (±2×Standard Errors).

Adult zebrafish right eyes were injected with 1 μL of 6 mg/mL of rose bengal and exposed to low or high doses of light. Each experiment was done in triplicate, so three retina samples from three different treatments were averaged, where each sample was compared to the uninjected eye of each fish as a control. The treated and untreated retina from each fish was collected as described at 2, 4, 6 hours after treatment and RNA samples were isolated using RNAeasy kit (Quiagen). cDNA was synthesized using RNeasy kit (Qiagen) and DNAase digested (Qiagen). cDNA was synthesized using Superscript II Reverse Transcriptase (Invitrogen) using oligo dT to prime the reactions. For real-time quantitative PCR analysis, the cDNAs were diluted 1:20, mixed with 1 μM of each primer and FastStart SYBR Green Mix (Roche). Amplifications were carried out on LightCycler480 (Roche) in triplicate. Ct values were normalized against *ribosomal protein p0* (*rppo*) and the average fold change in the three treated groups was compared to the values in the untreated controls. Genes involved in cellular stress response and transcription factors with a homeobox domain (Table 2) were analyzed by real-time quantitative PCR (qPCR).

3. Results

Two hour hematoxylin and eosin light microscopic histologic sections at low exposure (6 mg/mL, 1 μL intravitreal injection followed by 1 min of 37×10^3 lx) and high exposure (6 mg/mL 1 μL injection followed by 1 min of 83×10^3 lx) were obtained. Rod outer segment (ROS), cone nuclei (CN), rod nuclei (RN) and inner nuclear layer (INL) layers all showed statistically significant ($n=6$, $p<0.05$) increases in thickness compared with controls in both low and high exposures. In the 4 hour high exposure groups, the RPE, ROS, CN and INL demonstrated statistically significant increases ($p<0.05$ for all layers) in length relative to the control. In the low exposure groups the ROS and RN decreased in size, but the decrease was not statistically significant, while PG and CN decreases in size were statistically significant ($p<0.05$). The 4 hour low exposure had a statistically significant ($p<0.05$) increase in the INL (Figs. 1 and 2).

In addition to the increases in length in many of the retinal layers after 2 and 4 h low and high exposure lesions, thickening of the photoreceptors, cone and rod nuclei and ganglion cells was noted. The injection of 1 μL of Thiokynurenate immediately after low or high

exposures resulted in a diffuse compression of all the retinal layers in statistically significant manner ($p<0.05$) (Fig. 1G).

Ultrastructural analysis showed marked thickening of the ROS, rod and cone ellipsoids at high exposure and enlargement of the pigment granules of the retinal pigment epithelial cells at low exposure (Fig. 3). EM of the inhibitor 4 h after low exposure showed not only substantial reduction in size and thickness of the retinal layers, but also loosening of the ROS (see arrows in Fig. 4) and disarray of the membranes (arrow, Fig. 4C).

In order to examine whether rose bengal and light generated sufficient oxidative stress to alter the expression of *sod* and to induce ER stress, we carried out qPCR. Four hours following treatment, there was upregulation in *sod*, *bip* and *chop* suggesting oxidative and ER stress pathways (Fig. 5A).

Several homeobox genes have been demonstrated to be essential for retinal development (Raymond, Barthel, Bernardos, & Perkowski, 2006), and we hypothesized that these may be induced during retinal degeneration. We found that *rx1* was upregulated 4–6 h after low and high lesions, but *lhx2* and *pax6* showed only modest upregulation 4 h post-lesion (Fig. 5B). Interestingly, thiokynurenate treatment prevented upregulation of *pax6*, *lhx2*, and *chop* (Fig. 5C), but did not inhibit the expression of *sod*, *bip*, and *rx1*.

4. Discussion

Retinal degeneration is caused by a number of factors, including genetic predisposition and oxidative stress. We used adult zebrafish to develop a vertebrate experimental model of oxidative stress induced retinal degeneration that will be useful for investigating the molecular and genetic mechanisms that give rise to this disease.

We report that low and high doses of photochemical stress cause a mixed phenotype in zebrafish retinal layers at two and 4 h following injury. We believe that these represent progression of the disease. For instance, 2 h after photochemical damage, photoreceptors, pigment granules, rod and cone nuclei, and ganglion cells all showed graded enlargement and thickening. By 4 h after photochemical lesion, the low exposure showed approximately 20% enlargement of the INL ($p<0.05$) and the high exposure was characterized by marked ROS and INL enlargement and thickening. Prior studies of retinal exposure to polychlorinated biphenyls (PCBs) in zebrafish also illustrated photoreceptor elongation. Of interest, rose bengal, thyroid hormone and PCBs all contain polyiodinated phenyl groups, which based on their similarity in structure all penetrate the photoreceptor membranes quite readily (Lavakumar, 2003). This may have facilitated the early outer segment membrane elongation seen in this study on light and electron microscopy (Figs. 1C and 3C).

Several investigators have demonstrated that in mammals, restricted photochemical lesions in brain cortex and retina produce ischemia, which results in free radicals that damage the endothelium and cause thrombotic stroke (Moroni et al.,1993; Mosinger & Olney,1989; Royster et al., 1988). Additionally, photochemical stress with incremental dosages induced increasing mitochondrial instability, ischemia, apoptosis and/or necrosis (Sakharov, Bunschoten, van Weelden, & Wirtz, 2003; Zhang et al., 2005). In this study, the photoreceptor enlargement 2 h after low and high exposures, may have derived from the simple weakening of the photoreceptor membranes from lipid or protein peroxidation (Morgan, Dean, & Davies, 2002; Sakharov et al., 2003). We did not see any evidence of cell death in our studies. Our findings that *sod*, *bip* and *chop* are upregulated in a dose-dependent fashion are consistent with the hypothesis that we induced oxidative stress and cellular stress with our treatment. Additionally, our findings that some, but not all, homeobox genes that regulate retinal development (*rx1*, *lhx2* and *pax6*) are moderately induced by retinal damage

suggests that our model induces some retinal remodeling or regeneration, followed by more advanced apoptotic, ischemic and necrotic progression (Eichenbaum et al., 2002; Sakharov et al., 2003). It is also possible that the photochemical lesion itself could release high levels of glutamate, producing excitotoxic lesions that elongate and thicken the photo-receptors and their membranous outer segments. This is suggested from our finding of the substantial increase in *bip*, an ER stress sensor which is upregulated with the unfolded protein response (Gulow et al., 2002) (Fig. 5A). This may signify membrane alteration, cellular dysfunction and ultimate photoreceptor degeneration (Fadiel et al., 2007).

The photochemical retinal lesion of this study differed dramatically from our previous reports of ischemic, thrombotic infarct in the rat brain (Pevsner et al., 2001) and the rose bengal induced central retinal artery occlusion (Zhang et al., 2005). Each of these studies illustrated the vascular occlusive effects of the rose bengal/white light photo-chemical lesion. It is possible that because of lower light and rose bengal exposure, the zebrafish retina model represents cellular stress with pre-ischemic, membrane and mitochondrial alterations, rather than thrombotic changes. These changes are not unlike those seen in our murine brain photochemical lesion study (Eichenbaum et al., 2002) and the Lavakumar PCB retinal morphology (Lavakumar, 2003). Thus, the rose bengal photochemical lesion illustrates a spectrum of histopathologic consequences from frank thrombotic stroke to modest cellular retinal stress and photoreceptor elongation. The monitoring of phenomena such as ischemic preconditioning (Kamphuis, Dijk, & Bergen, 2007) and cellular adaptation to oxidative and cellular stress can now be improved using this zebrafish model.

The NMDA receptor may be an alternate mechanistic pathway in the rose bengal photochemical lesion. INL elongation was not appreciably altered in the high exposures with the addition of thiokynurenate. In the low exposure retinas, the inhibitor produced additional photoreceptor outer segment disarray. In contrast to the expansive photochemical stress lesion, the NMDA inhibitor produced a globally compressed retinal layer lesion. The photochemical process of focal ischemia, in chronology and morphology mimic the exposure to large concentrations of glutamate, which results in activation of the NMDA receptors. These receptors may be responsible for excitotoxic retinal neuronal death (Lombardi, Moroni, & Moroni, 1994; Moroni et al., 1993; Olney et al., 1986). A single intravitreal injection of excitatory amino receptor antagonist significantly reduced the loss of retinal neurons in mammals (Moroni et al., 1993). In contrast, we find that thiokynurenate did not reduce the photoreceptor elongation and thickening and inner plexiform vacuolation alterations, although gene expression analysis indicates that it reduced oxidative and cellular stress. The marked retinal layer compression observed in samples treated with thiokynurenate suggests multiple molecular pathways derive from the insult.

It has been suggested (Chen & Lipton, 2006) that NMDA receptors may exhibit several types of responses, relative to the level of excitotoxic lesion. For example, a surge of free radicals and glutamate may induce calcium channel overload, causing rescue pathways to either block calcium channels directly or via NMDA mediated calcium channel activity. Another explanation for this nonlinear effect in the low vs. high inhibitor effect on the retina may lie in the induction of free radicals by kynurenic acid itself (Darlington et al., 2007). Additional research is required to better understand the role of the NMDA receptor in this model.

5. Conclusion

Further investigation using the zebrafish model described herein provides a basis for studying the role of cellular stress and the genes that contribute to retinal degeneration.

Acknowledgments

Funding

Irene Duel Fund for Ophthalmologic Research, in honor of the late Dr. Duel, Mount Sinai School of Medicine, Department of Ophthalmology, NY, USA.

The authors wish to acknowledge help from: Smita Gopinath for gene expression; Noreen Mall for microscopic slides Joseph Samet for imaging; Dr. Ronald Gordon for EM; and Dr. Mihaly Mezei for statistical analysis, Mount Sinai School of Medicine, NY, USA.

References

Cao R, Jensen LD, Soll I, Hauptmann G, Cao Y. Hypoxia-induced retinal angiogenesis in zebrafish as a model to study retinopathy. PLoS ONE. 2008; 3(7):e2748. [PubMed: 18648503]

Chen HS, Lipton SA. The chemical biology of clinically tolerated NMDA receptor antagonists. Journal of Neurochemistry. 2006; 97(6):1611–1626. [PubMed: 16805772]

Darlington LG, Mackay GM, Forrest CM, Stoy N, George C, Stone TW. Altered kynurenine metabolism correlates with infarct volume in stroke. European Journal of Neuroscience. 2007; 26(8):2211–2221. [PubMed: 17892481]

Sheehan, DC.; Hrapchak, BB. Theory and practice of histopathology. 2. Pittsburgh: ThermoShandon Company; 1980. p. 142-143.

Eichenbaum JW, Pevsner PH, Pivawer G, Kleinman GM, Chiriboga L, Stern A, et al. A murine photochemical stroke model with histologic correlates of apoptotic and nonapoptotic mechanisms. Journal of pharmacological and toxicological methods. Journal of Pharmacological and Toxicological Methods. 2002; 47(2):67–71. [PubMed: 12459144]

Fadiel A, Eichenbaum KD, Hamza A, Tan O, Lee HH, Naftolin F. Modern pathology: protein mis-folding and mis-processing in complex disease. Current Protein and Peptide Science. 2007; 8(1):29–37. [PubMed: 17305558]

Gross JM, Perkins BD, Amsterdam A, Egana A, Darland T, Matsui JI, et al. Identification of zebrafish insertional mutants with defects in visual system development and function. Genetics. 2005; 170(1): 245–261. [PubMed: 15716491]

Gulow K, Bienert D, Haas IG. BiP is feed-back regulated by control of protein translation efficiency. Journal of Cell Science. 2002; 115(Pt 11):2443–2452. [PubMed: 12006628]

Haimovici R, Ciulla TA, Miller JW, Hasan T, Flotte TJ, Kenney AG, et al. Localization of rose bengal, aluminum phthalocyanine tetrasulfonate, and chlorin e6 in the rabbit eye. Retina. 2002; 22(1):65–74. [PubMed: 11884881]

Horibe T, Hoogenraad NJ. The *chop* gene contains an element for the positive regulation of the mitochondrial unfolded protein response. PLoS ONE. 2007; 2(9):e835. [PubMed: 17848986]

Kamphuis W, Dijk F, Bergen AA. Ischemic preconditioning alters the pattern of gene expression changes in response to full retinal ischemia. Molecular Vision. 2007; 13:1892–1901. [PubMed: 17960128]

Kassen SC, Ramanan V, Montgomery JE, Burket CT, Chang-Gong Liu Vihtelic T, et al. Time course analysis of gene expression during light-induced photoreceptor cell death and regeneration in albino zebrafish. Developments in Neurobiology. 2007; 67(8):1009–1031.

Lavakumar M. Changes in retina morphology in vertebrates following exposure to polychlorinated biphenyls. Journal of Undergraduate Research. 2003; 4(9)

Liu Q, Londraville RL. Using the adult zebrafish visual system to study cadherin-2 expression during central nervous system regeneration. Methods in Cell Science. 2003; 25(1–2):71–78. [PubMed: 14739590]

Lombardi G, Moroni F, Moroni F. Glutamate receptor antagonists protect against ischemia-induced retinal damage. European Journal of Pharmacology. 1994; 271(2–3):489–495. [PubMed: 7705449]

Malicki J, Neuhauss SC, Schier AF, Solnica-Krezel L, Stemple DL, Stainier DY, et al. Mutations affecting development of the zebrafish retina. Development. 1996; 123:263–273. [PubMed: 9007246]

Matini P, Moroni F, Lombardi G, Faussone-Pellegrini MS, Moroni F. Ultrastructural and biochemical studies on the neuroprotective effects of excitatory amino acid antagonists in the ischemic rat retina. Experimental Neurology. 1997; 146(2):419–434. [PubMed: 9270053]

Morgan PE, Dean RT, Davies MJ. Inhibition of glyceraldehyde-3-phosphate dehydrogenase by peptide and protein peroxides generated by singlet oxygen attack. European Journal of Biochemistry/FEBS. 2002; 269(7):1916–1925. [PubMed: 11952793]

Moroni F, Alesiani M, Facci L, Fadda E, Skaper SD, Galli A, et al. Thiokynurenates prevent excitotoxic neuronal death in vitro and in vivo by acting as glycine antagonists and as inhibitors of lipid peroxidation. European Journal of Pharmacology. 1992; 218(1):145–151. [PubMed: 1356805]

Moroni F, Alesiani M, Galli A, Mori F, Pecorari R, Carla V, et al. Thiokynurenates: a new group of antagonists of the glycine modulatory site of the NMDA receptor. European Journal of Pharmacology. 1991; 199(2):227–232. [PubMed: 1720099]

Moroni F, Lombardi G, Pellegrini-Faussone S, Moroni F. Photochemically-induced lesion of the rat retina: a quantitative model for the evaluation of ischemia-induced retinal damage. Vision Research. 1993; 33(14):1887–1891. [PubMed: 8249308]

Mosinger JL, Olney JW. Photothrombosis-induced ischemic neuronal degeneration in the rat retina. Experimental Neurology. 1989; 105(1):110–113. [PubMed: 2744125]

Olney JW. Glutaate-induced retinal degeneration in neonatal mice. Electron microscopy of the acutely evolving lesion. Journal of Neuropathology and Experimental Neurology. 1969; 28(3):455–474. [PubMed: 5788942]

Olney JW, Price MT, Fuller TA, Labruyere J, Samson L, Carpenter M, et al. The anti-excitotoxic effects of certain anesthetics, analgesics and sedative–hypnotics. Neuroscience Letters. 1986; 68(1):29–34. [PubMed: 3523314]

Pevsner PH, Eichenbaum JW, Miller DC, Pivawer G, Eichenbaum KD, Stern A, et al. A photothrombotic model of small early ischemic infarcts in the rat brain with histologic and MRI correlation. Journal of Pharmacological and Toxicological Methods. 2001; 45(3):227–233. [PubMed: 11755387]

Picaud S, Peichl L, Franceschini N. Dye-induced photolesion in the mammalian retina: glial and neuronal reactions. Journal of Neuroscience Research. 1993; 35(6):629–642. [PubMed: 8411266]

Raymond PA, Barthel LK, Bernardos RL, Perkowski JJ. Molecular characterization of retinal stem cells and their niches in adult zebrafish. BMC Developmental Biology. 2006; 6:36. [PubMed: 16872490]

Royster AJ, Nanda SK, Hatchell DL, Tiedeman JS, Dutton JJ, Hatchell MC. Photochemical initiation of thrombosis. Fluorescein angiographic, histologic, and ultrastructural alterations in the choroid, retinal pigment epithelium, and retina. Archives of Ophthalmology. 1988; 106(11):1608–1614. [PubMed: 3190547]

Sadda SR, Yu YS, de Juan E Jr, Rencs EV, Green WR, Gottsch JD. Photosensitization-induced retinopathy in the newborn beagle. Investigative Ophthalmology and Visual Science. 1994; 35(3):1202–1211. [PubMed: 8125731]

Sakharov DV, Bunschoten A, van Weelden H, Wirtz KW. Photodynamic treatment and H2O2-induced oxidative stress result in different patterns of cellular protein oxidation. European Journal of Biochemistry. 2003; 270(24):4859–4865. [PubMed: 14653812]

Vihtelic TS, Hyde DR. Light-induced rod and cone cell death and regeneration in the adult albino zebrafish (*Danio rerio*) retina. Journal of Neurobiology. 2000; 44(3):289–307. [PubMed: 10942883]

Wehman AM, Staub W, Meyers JR, Raymond PA, Baier H. Genetic dissection of the zebrafish retinal stem-cell compartment. Developmental Biology. 2005; 281(1):53–65. [PubMed: 15848388]

Westerfield, M. Zebrafish handbook. 1995.

Zhang Y, Cho CH, Atchaneeyasakul LO, McFarland T, Appukuttan B, Stout JT. Activation of the mitochondrial apoptotic pathway in a rat model of central retinal artery occlusion. Investigative Ophthalmology and Visual Science. 2005; 46(6):2133–2139. [PubMed: 15914634]

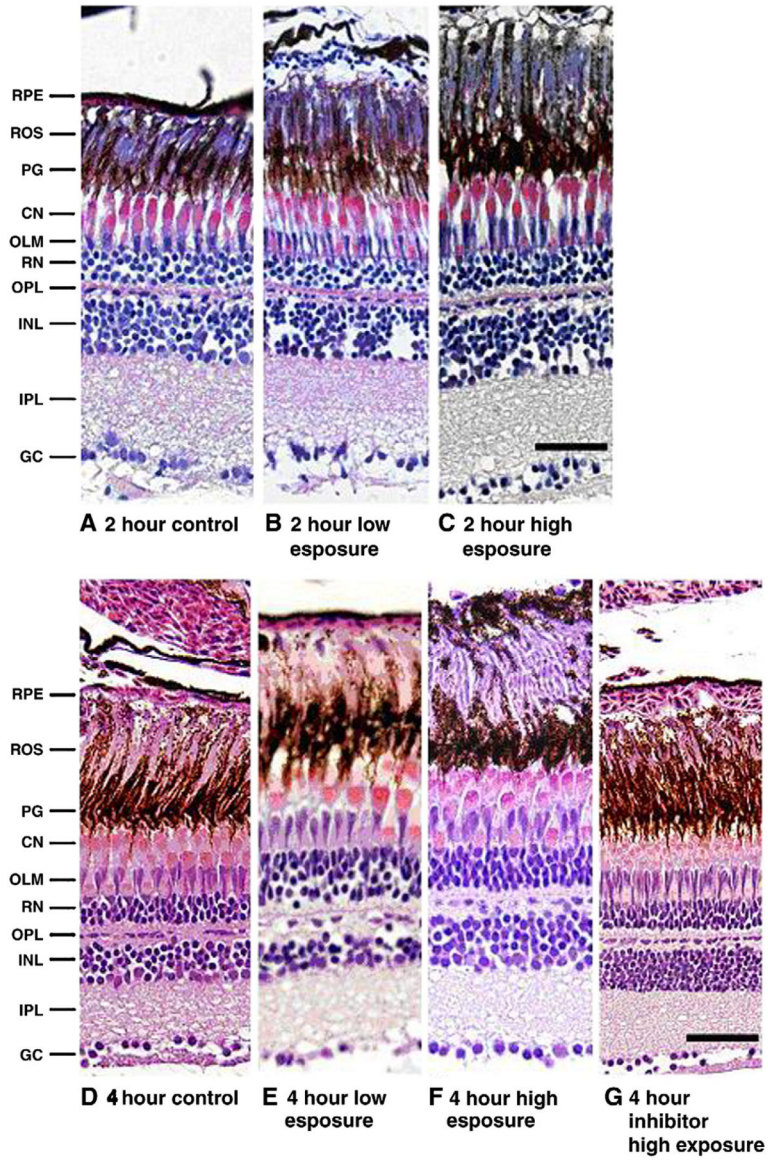

Fig. 1.

Graded zebrafish retinal oxidative stress. Composite of representative 400× hematoxylin and eosin slides of 2 and 4 h control and experimental exposures. *Key: RPE*, retinal pigment epithelium; *ROS*, rod outer segment; *PG*, pigment granules; *CN*, cone nuclei; *OLM*, outer limiting membrane; *RN*, rod nuclei, *OPL*, outer plexiform layer; *INL*, inner nuclear layer; *IPL*, inner plexiform layer; *GC*, ganglion cell layer. A. 2 h control retina without rose bengal light exposure. B. 2 h low exposure, 1 μL rose bengal intravitreal injection,6 mg/mL, followed by 1 min 37×10^3 lx. C. 2 h high exposure, 1 μL rose bengal intravitreal injection, 6 mg/mL, followed by 1 min 83×10^3 lx; note elongation of ROS in the low exposure (B) and the marked elongation of the ROS in the high exposure (C), as well as the elongation of the nuclear layers and inner plexiform layers in c. D. 4 h control retina without rose bengal or light exposure. E. 4 h low exposure. Note the thickening of the ROS, the nuclear layers and the IPL. F. 4 h high exposure. Note the thickening and elongation of the ROS, the nuclear layers, and the IPL and the ganglion cells. G. 4 h retina with 400 nm 1 μ thiokynurnenate NMDA inhibitor immediately after high exposure.

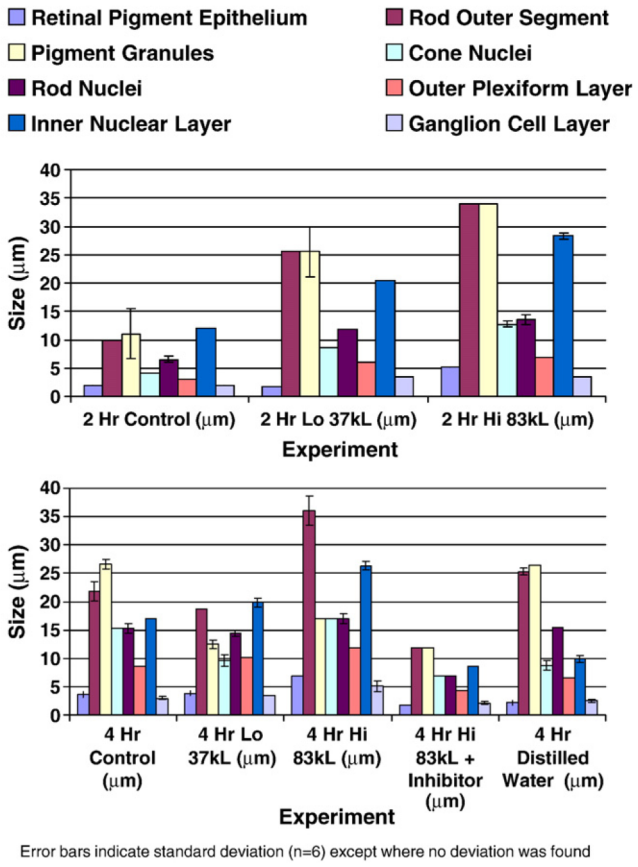

Fig. 2.

Histogram of retinal layer size in μm, vs. experimental exposure. *N*=6 for each experiment and the concentration of rose bengal was uniformly 1 μL, 6 mg/mL rose bengal intravitreally, followed by 1 min of cold white light in lux as listed.

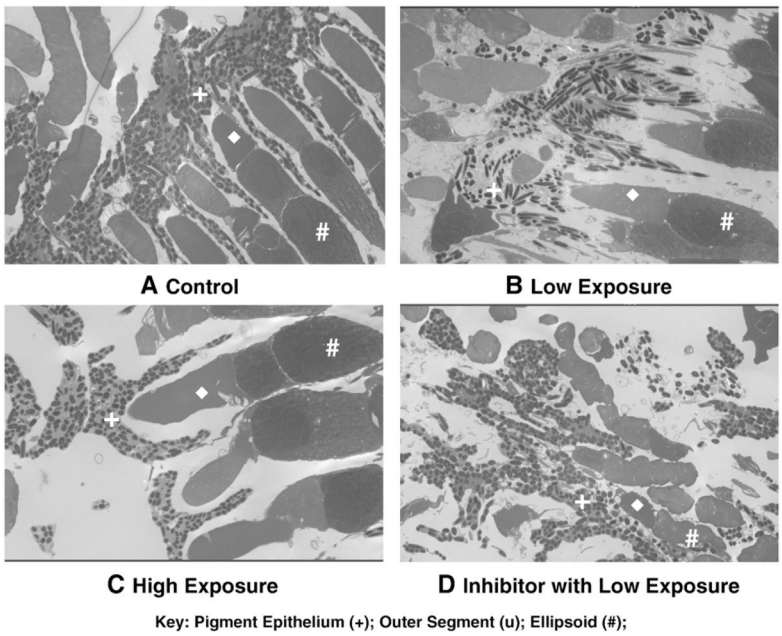

Fig. 3.

Electron micrographs of zebrafish retinae: magnification: 2500×. A: control retina; B: low exposure (37×103 lx, 6 mg/mL rose bengal) note: modest elongation of outer segment, diamond; C: high exposure (83×103 lx, 6 mg/mL rose bengal); note: pronounced elongation of outer segment, diamond D: inhibitor thiokynurnate 400 nM after 37×103 lx, 6 mg/mL rose bengal) note: marked reduction of outer segment, diamond, and ellipsoid, #.

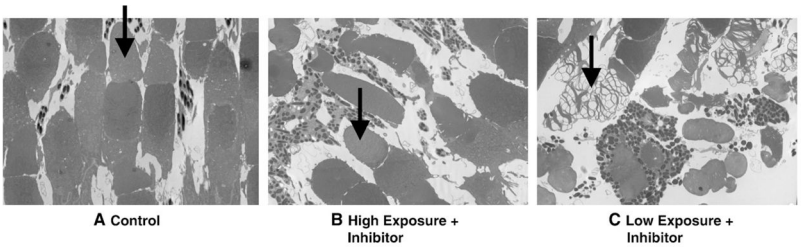

Fig. 4.

Electron micrograph of zebrafish retina outer segment. Note the disarray of low inhibitor outer segments (arrows) compared with compressed but organized High Inhibitor Outer Segments and Normal Controls.

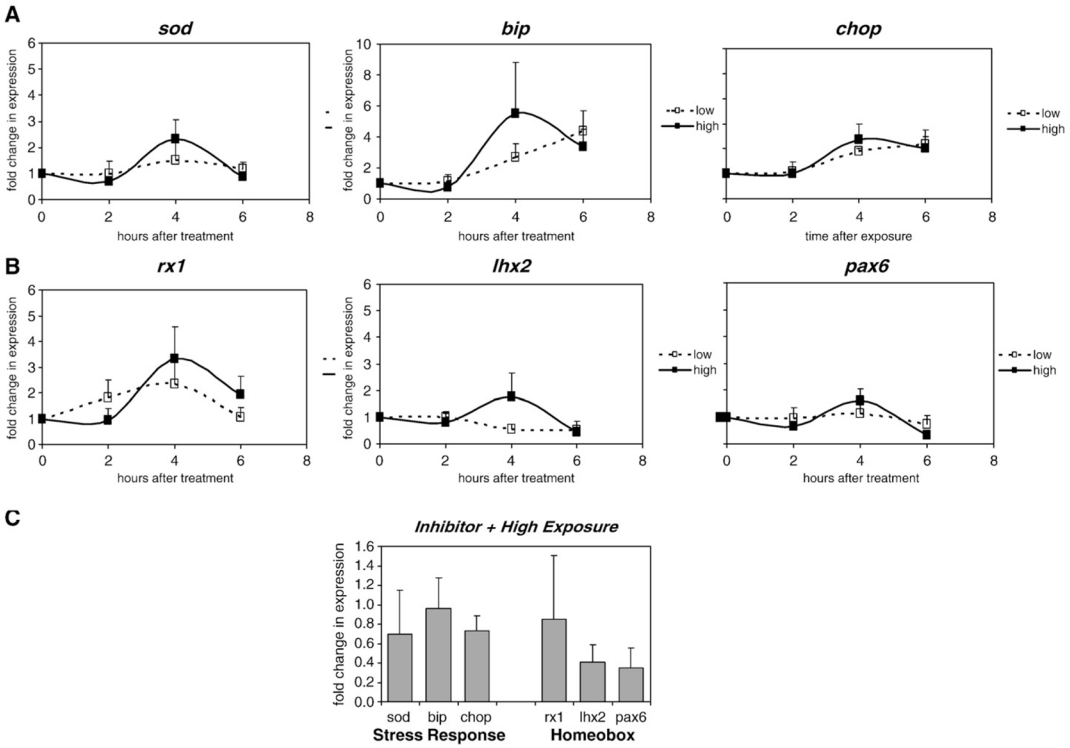

Fig. 5.

Selected gene changes from zebrafish retinal photochemical stress model. Photochemical induced change is captured in *sod*, *bip*, *chop* (A) and homeobox genes (B) as analyzed by real-time quantitative PCR. The NMDA inhibitor, thiokynurenate, generally demonstrated inhibition of *sod*, *bip*, and *chop*, as well as several of the homeobox genes (C). The expression levels in the treated eyes were normalized to that of the untreated. Values represent an average of 3 experiments, and error bars represent standard deviations.

Table 1

Experimental design: controls, experimental and inhibitor groups (*n*=6 per group).

	Duration (h)	Rose bengal	Light (lx)
Experiment: low exposure (37×10^3 lx) group			
Group 1	2	6 mg/mL	37×10^3
Group 2	2	12 mg/mL	37×10^3
Group 3	4	6 mg/mL	37×10^3
Group 4	4	12 mg/mL	37×10^3
Experiment: high exposure (83×10^3 lx) group			
Group 5	2	6 mg/mL	83×10^3
Group 6	2	12 mg/mL	83×10^3
Group 7	4	6 mg/mL	83×10^3
Group 8	4	12 mg/mL	83×10^3
Control groups			
Group 9	2	No	No
Group 10	2	No	37×10^3
Group 11	2	No	83×10^3
Group 12	4	No	37×10^3
Group 13	4	No	83×10^3
Group 14	2	6 mg/mL	No
Group 15	2	12 mg/mL	No
Group 16	4	6 mg/mL	No
Group 17	4	12 mg/mL	No
Group 18: saline intravitreal injection	4	No	No
Group 19: distilled water	4	No	No
Inhibitor groups			
Group 20: inhibitor alone	4	No	No
Group 21: inhibitor	4	6 mg/mL	37×10^3
Group 21: inhibitor	4	6 mg/mL	83×10^3

Table 2

Primers used.

sod 1-F	AGCCCCATTATGCTGTGAAC
sod 1-R	TCGGGAAGGTTGATTTTCAG
bip-F:	AAGAGGCCGAAGAGAAGGAC
bip-R:	AGCAGCAGAGCCTCGAAATA
chop-F:	AAGGAAAGTGCAGGAGCTGA
chop-R:	TCACGCTCTCCACAAGAAGA
rx1-F	AGCTGTCTTTCGCCCAGTAA
rx1-R	ACGAATCCTGGTCCTTGTTG
lhx2-F	TCAGACCGATCAGACACTGC
lhx2-R	ATATGCACGTGTTTCCGTCA
pax6-F	CTGACGTTTTTGCACGAGAA
pax6-R	AACTTTTCCTCCCTCCTCCA